EFFECT OF ARTIFICIALLY PRODUCED PIT-LIKE DEFECTS ON THE STRENGTH OF AISI 410 STAINLESS STEEL COMPRESSOR BLADES

M. A. Khattak[a]*, Mazmir Mat Noh[a], M. N. Tamin[a], Nida Iqbal[b], Amir Husni Muhd Syariff[b], S. Kazi[c], Mohd Hafiz Abdul Ghaffar[d]

[a]Department of Applied Mechanics and Design, Faculty of Mechanical Engineering, Universiti Teknologi Malaysia, 81310 UTM Johor Bahru, Johor, Malaysia
[b]Medical Devices & Technology Group (MEDITEG), Faculty of Biosciences and Medical Engineering, Universiti Teknologi Malaysia, 81310 UTM Johor Bahru, Johor, Malaysia
[c]Faculty of Engineering, Islamic University of Madinah, Prince Naif Ibn Abdulaziz, Al Jamiah 42351, Medinah, Saudi Arabia
[d]Materials Engineering Group, TNB Research Sdn Bhd, Bandar Baru Bangi, 43000 Kajang, Selangor, Malaysia

*Corresponding author
muhdadil@utm.my

Abstract

In the present paper, the effect of artificially produced pit-like defects on the strength of members made of AISI 410 martensitic stainless steel were investigated. Compressor blades in power generation industries made of AISI 410 stainless steel commonly suffer from pitting corrosion. Well-defined pit-like defects were artificially produced on various specimen and strength tests were conducted. AISI 410 stainless steel microstructure shows a typical body-centered tetragonal (bct) structure. Strength tests analysis established yield strength of 547 MPa for Case 1 (max depth-max diameter) whereas a yield strength of 585 MPa for Case 2 (min depth-min diameter). In addition, strength and elongation of the artificially produced pitted tensile specimen gradually decrease with the increase of the area lost due to artificially produced pits.

Keywords: Stainless steel, compressor blades, pitting, strength

1.0 INTRODUCTION

Fatigue failure originating from pitting corrosion has been identified as one of the dominant life-limiting factors for gas turbine blades [1-6]. In power generation industries, compressor blades are subjected to corrosive environment from the incoming air during the operation [7]. In this respect, the effects of pitting corrosion on the structural strength and the integrity of the compressor blades need to be established. Nakai *et al.* [8] has concluded that the nominal tensile strength of pitted structural members decreases gradually while the total elongation decreases drastically with the increase of thickness loss due to pitting. Yoshino and Ikegaya [9] found that even small amount of H2S have a significant detrimental effect on the resistance of the steels to the pitting corrosion in his study on 12Cr-Ni-Mo martensitic stainless steel in chloride and sulfide environments.

Geometric discontinuity due to a pit induces a large stress gradient with high magnitude of localized stress [10-12]. The time to nucleate a corrosion pit under surface straining was analyzed at the microscale [13]. A relationship between surface stress and pitting corrosion has been established [14]. The effect of pitting damage is to reduce the life of structural components [6, 15-20]. Earlier research has already established pits geometry details [21]. This

research examines the strength response of AISI 410 martensitic stainless steel compressor blade material with different geometries of artificially produced pit-like defects. Several cases using same specimen geometry but different artificial pit geometries has been examined. The yield strength of the stainless steel sample coupons with and without artificial pit is compared.

2.0 EXPERIMENTAL

2.1 Material

The material employed in this study is an AISI 410 martensitic stainless steel. The material was received in the form of circular plate with radius and thickness of 440 and 18 mm, respectively. For microstructural study, the specimens were finely grind, polished and etched in the etching solution (5 ml HCl + 2 gr Picric acid + 100 ml Ethyl alcohol) for approximately 7 seconds and examined using optical microscope. For quantifying the duration of specimen immersion time to produce desirable pits, the material was wire-cut using Electrical Discharge Machine (EDM) into samples at 20 x 10 x 2 mm3. Dog-bone shaped specimens, with dimensions based on ASTM A370 standards were machined for use in tensile test. Figure 1 illustrates the dimension details of the tensile specimen used with a gage length of 25 mm.
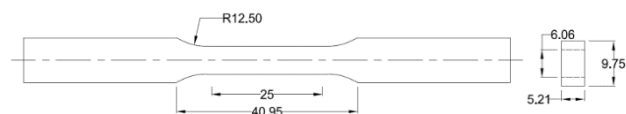
Figure 1 Geometry of the tensile specimen (all dimensions in mm)

Mechanical and chemical composition of the material are shown in Table 1 and 2. The primary alloying elements are chromium and carbon. The chromium provides the excellent corrosion resistant or stainless property while carbon defines the strength of the steel.. Manganese and nickel contribute to improved toughness of the steel.

Table 1 Chemical composition of AISI 410 steel [21]

Chemical	Weight Percentage (wt %)
C	0.2
Mn	0.5
P	0.02
S	0.002
Si	0.35
Cr	14.20
Ni	0.39
Mo	0.01
Al	0.003
V	0.03
Fe	Bal.

Table 2 Mechanical properties of AISI 410 steel at room temperature [21]

Tensile Strength (MPa)	Yield Strength (MPa)	Elongation (pct.)	Maximum Load (kN)
656.04	620.17	30	21.27

2.2 Microstructure

For microstructural study, the specimens were finely grind, polished and etched in the etching solution (5 ml HCl + 2 gr Picric acid + 100 ml Ethyl alcohol) for approximately 7 seconds and examined using optical microscope. Figure 2 shows typical microstructures of the AISI 410 martensitic stainless steels at the three different orthogonal section planes. The microstructure shows a typical body-centered tetragonal (bct) structure. The dark area represents martensitic phase while light area the ferrite phase. The structure shows the matrix of equiaxed ferrite grains, with randomly dispersed particles of chromium carbide. Since qualitatively identical microstructure is displayed for each section, the material is expected to behave in isotropic manner.

2.3 Pitting Corrosion Experiment

Pitting corrosion experiment was performed using 6 pct. (by mass) of Ferric Chloride solution, $FeCl_3$ according to ASTM G48-11. This experiment was conducted at room temperature to quantify specimen immersion time for creating the desired characteristic corrosion pit morphology.

Three specimens were polished to 120-grit, cleaned with magnesium oxide paste, rinsed, dipped in methanol before air dried and finally immersed into Ferric Chloride solution. Each specimen was removed from the solution every 24 hours, rinsed thoroughly and finely scrubbed with nylon bristle brush under running water to remove corrosion particles. The specimen was then examined using optical microscope for pits. All specimens show different geometry and size of pits.

The pit geometry was quantified and compared with the measured geometry details on pitted blades of a retired compressor from a local power generation plant. An immersion time of 48 hours were selected on the basis of the above observation to produce the desired pitted morphology on the specimen.

2.4 Test Specimen

The dog-bone shaped specimens are used for tensile tests. After wire-cut using EDM, the specimens were grind and polished with abrasive paper before being stress-relief annealed in high vacuum at 106 Pa (heating from room temperature to 600 °C in 1 hour, holding for 2 hours, cooling from 600 °C to 400 °C in 2

hours and to room temperature in approximately 12 hours) to eliminate residual stresses [13].

To study the effect of different geometry pit-like defect on the strength of the material, artificial pit were generated in the gage length of the specimen. The maximum, minimum and nominal pit geometry details has been acquired from the earlier established research [21]. The artificial pits were generated using AG40L CNC Sinker EDM machine.
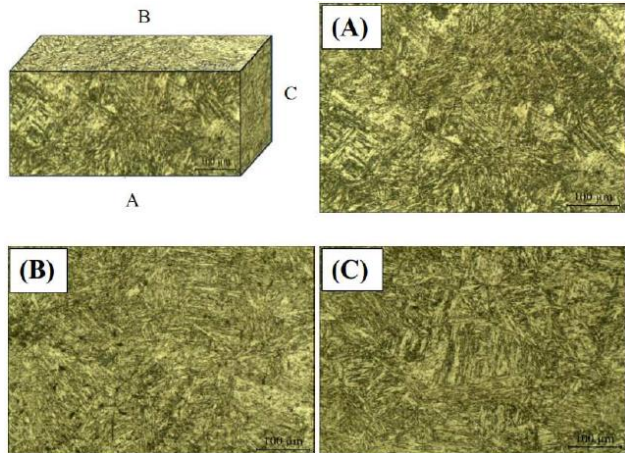
Figure 2 Microstructure observations for section A, B and C

The tensile specimen surface for the as-received and the pitted condition is compared in Figure 3. The grip area of the specimen is coated using epoxy-based enamel paint to yield preferred localized pitting at gage area. Tensile tests to fracture were performed using Instron electromechanical testing machine on both the as-received and pitted specimens. The displacement rate for the tensile test was set at 0.1 mm/min. since the cross-section area of the pitted specimen varies throughout the gage length, the extensometer is not used during the test.

Figure 3 (A) As-received and (B) corrosion pitted tensile specimen

3.0 RESULTS AND DISCUSSION

3.1 Pits Geometry Analysis

The geometry of the pits, in term of equivalent diameter and depthis analyzed statistically. More than 300 depth and diameter measurements were taken using PJ300 Mitutoyo Profile projector machine for diameter and CS5000 Mitutoyo Formtracer for depth measurements, respectively. The distribution of pit depths and diameters is shown in Figure 4 and Figure 5, respectively. Results show that the three sizes of the pits, 0.5, 0.6 and 0.9 mm are dominant. However, in view of localized stress concentration, the smallest diameter pit at 0.4 mm could be detrimental for crack initiation. In addition, the combination of the smallest diameter and deepest pit, at 0.26 mm from Figure 5 is the most critical geometry with respect to crack initiation and subsequent fatigue crack growth of the blade. Based on the experimental procedures described above, nominal depth of the pits is at 0.06 mm. The maximum, minimum and nominal pit diameter and depth values are listed in Table 3.
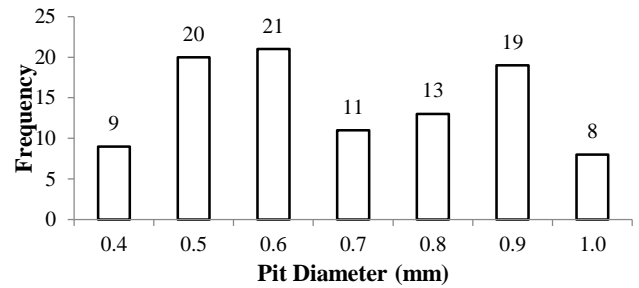
Figure 4 Pit diameter from corroded tensile specimen
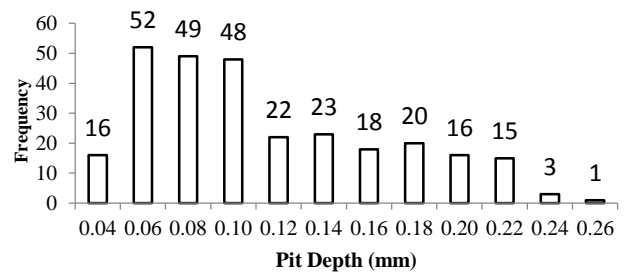
Figure 5 Pit depth from corroded tensile specimen

Table 3 Artificial pit geometry details

Geometry	Pit Diameter (mm)	Pit Depth (mm)
Maximum	1.00	0.75
Minimum	0.30	0.30
Nominal	0.50	0.50

3.2 Tensile Test Results

The resulting load-displacement yield strength values for as-received (AR) and artificially produced pitted specimen is compared in Figure 6. Results show that the apparent strength behavior of the pitted specimens of both geometry is lower than that of the AR specimen. The strength of specimen with minimum diameter and depth of artificial pit is 585 MPa, which is higher than the specimen with maximum diameter and depth of artificial pit, which is 547 MPa. This is due to the geometry of the artificial pit itself. Larger artificial pit size gives more impact on strength reduction of the specimen and translates into lower apparent yield strength. The observed behavior of lower load could be attributed to localized stress around the pits that leads to early failure of the material. Such localized failure manifests in the early and gradual degradation of stiffness of the pitted material, as shown in Figure 7.
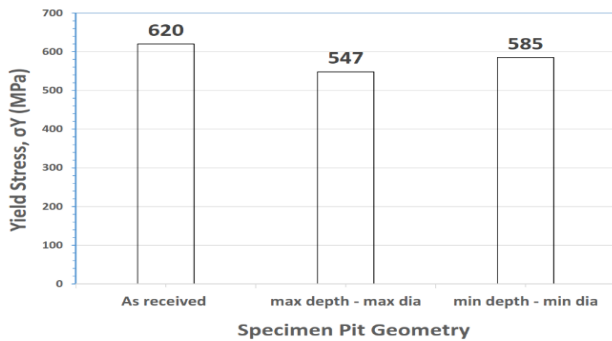
Figure 6 Yield stress values for artificially produced pitted specimen
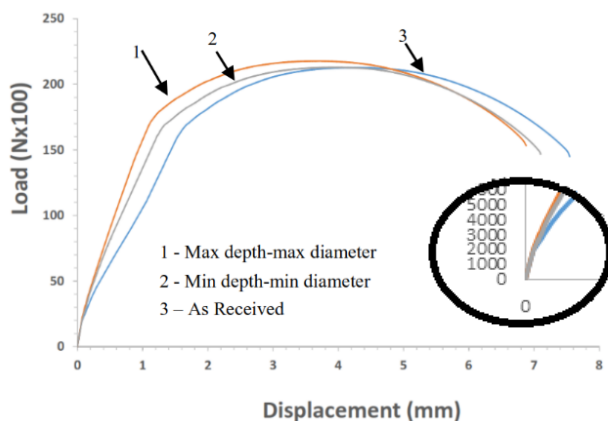
Figure 7 Tensile curves for as-received and artificially produced pitted specimen with enlarge view

A decrease in total elongation of the pitted compared to AR specimens is noted. Since the artificially produced pit area was selective and limited to the surface only, the apparent loss for elongation at fracture is likely due to the same effect

of localized stress at the pits, rather than degradation of ductility in the bulk section of the specimen.

4.0 CONCLUSION

Effects of different geometries of artificially produced pits on the apparent tensile behavior of AISI 410 martensitic stainless steel for compressor blades has been established. Major conclusions are as follows:

1. The strength of the material gradually decrease with the existence of the artificial pit.
2. The strength of the specimen with maximum diameter and depth of pit is lower than the strength of the specimen with minimum diameter and depth pit.
3. Depth of the pit gives more effect on the strength of the material. The deeper the depth of the pit, the weaker the strength of the material.
4. Immersion of AISI 410 stainless steel specimen in $FeCl_3$ solution (6 pct. By mass) for 48 hours could produce characteristic corrosion pits as found on compressor blades.
5. Although the nominal pit depth is 0.06 mm, combination of the smallest diameter (0.4 mm) and deepest pit (0.26 mm) is most critical with respect to fatigue crack initiation.

Acknowledgement

References

[1] Linden, D. 2011. Long Term Operating Experience With Corrosion Control in Industrial Axial Flow Compressors. *Proceedings of 14th Turbomachinery Symposium*. 12-15.
[2] Zhang, Y., *et al.* 2006. Passivity Breakdown On AISI Type 403 Stainless Steel In Chloride-Containing Borate Buffer Solution. *Corrosion Science*. 48(11): 3812-3823.
[3] Zhou, S. and A. Turnbull. 2003. Overview Steam turbines: Part 1–Operating Conditions And Impurities In Condensates, Liquid Films And Deposits. *Corrosion Engineering, Science and Technology*. 38(2): 97-111.
[4] Jonas, O. and J. M. Mancini. 2001. Steam Turbine Problems And Their Field Monitoring. *Materials Performance.* 40(3): 48-53.
[5] Schönbauer, B. M., *et al.* 2015. The Influence Of Corrosion Pits On The Fatigue Life Of 17-4PH Steam Turbine Blade Steel. *Engineering Fracture Mechanics*. 147: 158-175.
[6] Bhandari, J., *et al.* 2015. Modelling Of Pitting Corrosion In Marine And Offshore Steel Structures–A Technical Review. *Journal of Loss Prevention in the Process Industries*. 37: 39-62.
[7] Horner, D., *et al.* 2011. Novel Images Of The Evolution Of Stress Corrosion Cracks From Corrosion Pits. *Corrosion Science*. 53(11): 3466-3485.

[8] Nakai, T., *et al*. 2004. Effect Of Pitting Corrosion On Local Strength Of Hold Frames Of Bulk Carriers (1st report). *Marine Structures.* 17(5): 403-432.

[9] Yoshino, Y. and A. Ikegaya. 1985. Pitting and Stress Cracking of 12Cr-Ni-Mo Martensitic Stainless Steels in Chloride and Sulfide Environments. *Corrosion.* 41(2): 105-113.

[10] Cerit, M. 2013. Numerical Investigation On Torsional Stress Concentration Factor At The Semi Elliptical Corrosion Pit. *Corrosion Science.* 67: 225-232.

[11] Mu, Z. T., *et al*. 2011. The Stress Concentration Factor of Different Corrosion Pits Shape. *Advanced Materials Research*. Trans Tech Publ.

[12] Turnbull, A., L. Wright, and L. Crocker. 2010. New Insight Into The Pit-To-Crack Transition From Finite Element Analysis Of The Stress And Strain Distribution Around A Corrosion Pit. *Corrosion Science.* 52(4): 1492-1498.

[13] Vignal, V., *et al*. 2004. Influence Of Elastic Deformation On Initiation Of Pits On Duplex Stainless Steels. *Electrochemical And Solid-State Letters.* 7(4): C39-C42.

[14] Oltra, R. and V. Vignal. 2007. Recent Advances In Local Probe Techniques In Corrosion Research–Analysis Of The Role Of Stress On Pitting Sensitivity. *Corrosion Science*. 49(1): 158-165.

[15] Tousek, J. 1985. Theoretical Aspects Of The Localized Corrosion Of Metals.

[16] Rajasankar, J. and N. R. Iyer. 2006. A Probability-Based Model For Growth Of Corrosion Pits In Aluminium Alloys. *Engineering Fracture Mechanics.* 73(5): 553-570.

[17] Wu, H., *et al*. 2015. Crack Initiation Mechanism of Z3CN20.09M Duplex Stainless Steel during Corrosion Fatigue in Water and Air at 290° C. *Journal of Materials Science & Technology.* 31(11): 1144-1150.

[18] Xu, S.-h. 2015. Estimating The Effects Of Corrosion Pits On The Fatigue Life Of Steel Plate Based On The 3D Profile. *International Journal of Fatigue.* 72: 27-41.

[19] Shekhter, A., *et al*. 2015. The Effect Of Pitting Corrosion On The Safe-Life Prediction Of The Royal Australian Air Force P-3C Orion Aircraft. *Engineering Failure Analysis.*

[20] Fernandez, I., J. M. Bairán, and A. R. Marí. 2015. Corrosion Effects On The Mechanical Properties Of Reinforcing Steel Bars. Fatigue And Σ–E Behavior. *Construction and Building Materials.* 101: 772-783.

[21] Mat Noh, M., *et al*. 2014. Effect of Pitting Corrosion on Strength of AISI 410 Stainless Steel Compressor Blades. *Applied Mechanics and Materials*. Trans Tech Publ.